Achieving steady-state entanglement of remote micromechanical oscillators by cascaded cavity coupling

Huatang Tan,[1,*] L. F. Buchmann,[2] H. Seok,[2] and Gaoxiang Li[1]
[1]*Department of Physics, Huazhong Normal University, Wuhan 430079, China*
[2]*B2 Institute, Department of Physics and College of Optical Sciences, University of Arizona, Tucson, Arizona 85721, USA*
(Received 15 October 2012; published 14 February 2013)

In this paper, we propose a scheme for generating steady-state entanglement of remote micromechanical oscillators in unidirectionally coupled cavities. For the system of two mechanical oscillators, we show that when two cavity modes in each cavity are driven at red- and blue-detuned sidebands, respectively, a stationary two-mode squeezed vacuum state of the two mechanical oscillators can be generated by the cascaded cavity coupling. The degree of squeezing is controllable by adjusting the relative strength of the pump lasers. Our calculations also show that the achieved mechanical entanglement is robust against thermal fluctuations. For the case of multiple mechanical oscillators, we find that steady-state genuine multipartite entanglement can also be built up among the remote mechanical oscillators. The present scheme does not require nonclassical light input or conditional quantum measurements, and it can be realized with current experimental technology.

DOI: 10.1103/PhysRevA.87.022318 PACS number(s): 03.67.Bg, 42.50.Dv, 42.50.Wk

I. INTRODUCTION

Besides the fundamental research interest in quantum physics [1], realizing quantum effects of macroscopic objects is crucial for potential applications in ultrahigh-precision measurements and quantum information processing [2–4]. Thanks to the recent achievements in ground-state cooling of micromechanical oscillators via optomechanical coupling [5–8], the emerging field of cavity optomechanics as an interface between mechanical systems and optical field has become a unique platform to study quantum behavior of macroscopic mechanical systems [9–16]. Using well-established quantum optical techniques, optomechanics holds the promise to effectively prepare and manipulate nonclassical mechanical states.

Several schemes have been proposed to establish entanglement between a mechanical element and the driven cavity field or between vibrating membranes or end mirrors [17–21] by optomechanics. Especially, remote entanglement between two micromechanical oscillators in separated cavities via injecting squeezed light or conditional quantum measurements is investigated [22–24]. Also, it was shown that weak mechanical entanglement between two distant optomechanical oscillators can possibly be achieved merely by optomechanical coupling [25]. The entanglement of remote mechanical elements is of importance for constructing long-distance quantum communication networks [26].

On the other hand, generating quantum states by quantum-reservoir engineering has attracted a lot of attention recently. In this approach, the interaction between system and environment is engineered in such a way that the system relaxes into a desired state. The resulting quantum states are steady, independent of initial conditions, and, most importantly, robust against incoherent noise. To date, several schemes have been proposed to prepare entangled states of atomic systems by quantum dissipation [27–33], and moreover, the dissipative creation of steady-state entanglement between two separated atomic ensembles has been experimentally realized [34].

In this paper, we consider the generation of steady-state entanglement of remote micromechanical oscillators (membranes) by cascaded cavity coupling. We at first investigate the entanglement between two micromechanical membrane oscillators in a cascaded cavity system. In each cavity, a membrane oscillator is coupled to two nondegenerate cavity modes via parametric and beam-splitter-like interactions by driving the relevant cavity modes on blue- and red-detuned sidebands, respectively. For negligible mechanical damping, we find that the cavity dissipation can pull the two distant mechanical oscillators into a stationary two-mode squeezed vacuum. It is also shown that the two-mode entanglement is robust against thermal fluctuations when one takes into account the mechanical damping. We then extend the two-mode mechanical model to the case of multiple mechanical oscillators in an array of cascaded cavities. We show that in this system genuine multipartite steady-state entanglement can be built up among the remote mechanical oscillators via the cascaded cavity coupling.

The remainder of this paper proceeds as follows. In Sec. II, the model of a two-cascaded-cavity optomechanical system is introduced and the steady-state entanglement between the mechanical oscillators is investigated in detail. In Sec. III, we extend the previous model to the case of multiple mechanical oscillators in an array of unidirectionally coupled cavities and discuss the generation of multipartite entanglement among multiple mechanical oscillators. Finally, we give the conclusion in Sec. IV.

II. ENTANGLEMENT OF TWO MECHANICAL OSCILLATORS

A. Model and equations

As shown schematically in Fig. 1, we investigate a system consisting of two identical optical cavities connected by unidirectional coupling [35]. In each cavity, two driven cavity modes are coupled to a vibrating membrane via radiation pressure [36,37]. The role of the membranes could also be played by other mechanical systems such as trapped clouds of

*tanhuatang@phy.ccnu.edu.cn

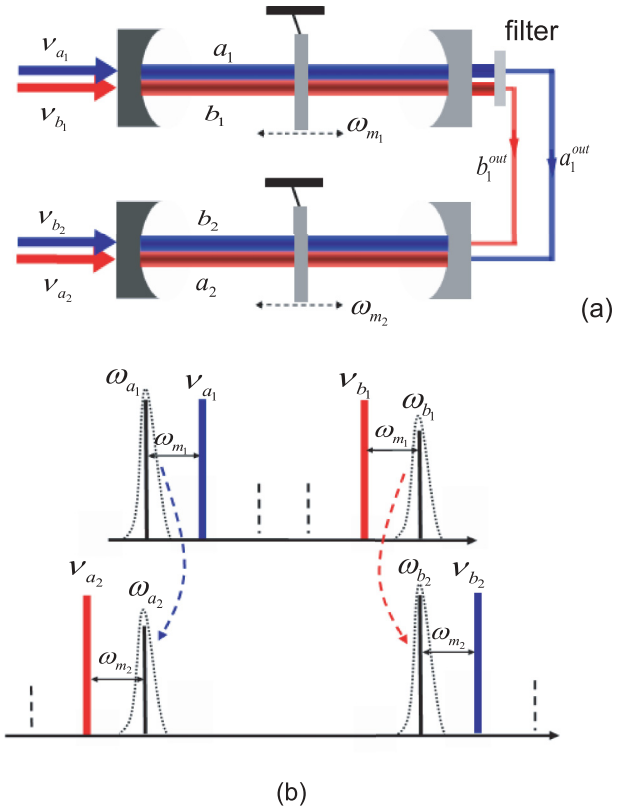

FIG. 1. (Color online) (a) Schematic setup of two-cascaded-cavity optomechanical system. In each cavity, two cavity modes are driven by red- and blue-detuned lasers, respectively, and the output quantum fluctuations from the first cavity are directed to the second cavity to drive the corresponding cavity modes. (b) Frequencies of the pumps and cavity modes; dashed arrows represent the unidirectional coupling between the cavity modes.

ultracold atoms [38]. After removing the carrier photons with filters, the output quantum fluctuations from the first cavity are directed to the second cavity to drive the corresponding cavity modes. With the light fields rotating at their driving frequencies, the Hamiltonian of the system is given by

$$H = \sum_{j=1,2} [\delta_{a_j} a_j^\dagger a_j + \delta_{b_j} b_j^\dagger b_j + \omega_{m_j} c_j^\dagger c_j + (\tilde{g}_{a_j} a_j^\dagger a_j + \tilde{g}_{b_j} b_j^\dagger b_j)(c_j + c_j^\dagger) + i(\mathcal{E}_{a_j} a_j^\dagger - \mathcal{E}_{a_j}^* a_j) + i(\mathcal{E}_{b_j} b_j^\dagger - \mathcal{E}_{b_j}^* b_j)], \quad (1)$$

where $a_j(a_j^\dagger)$ and $b_j(b_j^\dagger)$ $(j = 1,2)$ are annihilation (creation) operators for the cavity modes and $c_j(c_j^\dagger)$ for the mechanical modes of the vibrating membranes of frequencies ω_{m_j} in each cavity. The cavity-laser detunings $\delta_{z_j} = \omega_{z_j} - \nu_{z_j} (z = a,b)$, with ω_{z_j} being the cavity resonant frequencies and ν_{z_j} the corresponding driving frequencies. The optomechanical couplings are denoted $\tilde{g}_{z_j}$ and the amplitudes of the driving lasers $|\mathcal{E}_{z_j}| = \sqrt{2P_{z_j}\tilde{\kappa}_{z_j}/\hbar\nu_{z_j}}$, where P_{z_j} are the powers of the pump lasers and $\tilde{\kappa}_{z_j}$ the cavity loss rates of the left cavity mirrors.

We expand the quantum operators as $o_j = \bar{o}_j^s + \delta o_j$, where $\bar{o}_j^s$ are the steady-state classical amplitudes and δo_j the corresponding quantum fluctuation operators. By taking into account cavity losses and mechanical damping, the classical amplitudes are obtained as $\bar{z}_j^s = \mathcal{E}_{z_j}/(\kappa_{z_j} + i\Delta_{z_j})$ and $\bar{c}_j^s = \sum_z \tilde{g}_{z_j}|\bar{z}_j^s|^2/(\omega_{m_j} + i\gamma_{m_j})$, where $\Delta_{z_j} = \delta_{z_j} + 2\tilde{g}_{z_j}\mathrm{Re}(\bar{c}_j^s)$ and κ_{z_j} are the cavity loss rates from the output mirrors on the right of the cavities, and γ_{m_j} are the mechanical damping rates. Note that here we have assumed the cavity loss rates $\kappa_{z_j} \gg \tilde{\kappa}_{z_j}$ such that losses from the left cavity mirrors can be neglected. For intense driving fields we have $|\bar{o}_j^s|^2 \gg \langle \delta o_j^\dagger \delta o_j \rangle$ and Hamiltonian (1) can be linearized. Then by dropping the symbol "δ" in the fluctuation operators for simplicity of notation, the resulting Langevin equations of motion for the quantum fluctuations of the cavity and mechanical modes are obtained as

$$\begin{aligned}
\dot{a}_j &= -(\kappa_{a_j} + i\Delta_{a_j})a_j - ig_{a_j}(c_j + c_j^\dagger) + \sqrt{2\kappa_{a_j}}a_j^{\mathrm{in}}(t),\\
\dot{b}_j &= -(\kappa_{b_j} + i\Delta_{b_j})b_j - ig_{b_j}(c_j + c_j^\dagger) + \sqrt{2\kappa_{b_j}}b_j^{\mathrm{in}}(t),\\
\dot{c}_j &= -(\gamma_{m_j} + i\omega_{m_j})c_j - ig_{a_j}(a_j + a_j^\dagger) - ig_{b_j}(b_j + b_j^\dagger)\\
&\quad + \sqrt{2\gamma_{m_j}}c_j^{\mathrm{in}}(t), \qquad (2)
\end{aligned}$$

where the effective optomechanical coupling $g_{z_j} = |\bar{z}_j^s|\tilde{g}_{a_j} (z = a,b)$. The noise operators $a_1^{\mathrm{in}}(t)$ and $b_1^{\mathrm{in}}(t)$ describe the vacuum inputs to the first cavity and satisfy nonzero correlations $\langle a_1^{\mathrm{in}}(t)a_1^{\mathrm{in}\dagger}(t')\rangle = \delta(t - t')$ and $\langle b_1^{\mathrm{in}}(t)b_1^{\mathrm{in}\dagger}(t')\rangle = \delta(t - t')$. The input noise of the second cavity, characterized by the operators $a_2^{\mathrm{in}}(t)$ and $b_2^{\mathrm{in}}(t)$, are from the output fluctuations of the first cavity and transmission losses in the coupling. When the output quantum field of the cavity mode $a_1(b_1)$ is used to drive the cavity mode $a_2(b_2)$, then one has

$$a_2^{\mathrm{in}}(t) = \sqrt{\eta_a}\left[a_1^{\mathrm{in}}(t) - \sqrt{2\kappa_{a_1}}a_1(t)\right]e^{-i(\nu_{a_1} - \nu_{a_2})t} + \sqrt{(1 - \eta_a)}\tilde{a}_2^{\mathrm{in}}(t), \quad (3a)$$

$$b_2^{\mathrm{in}}(t) = \sqrt{\eta_b}\left[b_1^{\mathrm{in}}(t) - \sqrt{2\kappa_{b_1}}b_1(t)\right]e^{-i(\nu_{b_1} - \nu_{b_2})t} + \sqrt{(1 - \eta_b)}\tilde{b}_2^{\mathrm{in}}(t), \quad (3b)$$

where $\eta_z \in [0,1]$ $(z = a,b)$ accounts for the imperfect couplings between the two cavities. The operators $\tilde{a}_2^{\mathrm{in}}(t)$ and $\tilde{b}_2^{\mathrm{in}}(t)$ denote the local vacuum noise input to the second cavity. The parameter $\eta_z = 1$ corresponds to a lossless unidirectional coupling between the two cavities, whereas $\eta_z = 0$ describes two independent cavities. Note here that the exponential factors in the above equations result from the differences between the frequencies of the relevant pump lasers. In addition, $c_j^{\mathrm{in}}(t)$ are noise operators of the mechanical oscillators which have nonzero correlations $\langle c_j^{\mathrm{in}\dagger}(t)c_j^{\mathrm{in}}(t')\rangle = \bar{n}_{\mathrm{th}}^j\delta(t - t')$ and $\langle c_j^{\mathrm{in}}(t)c_j^{\mathrm{in}\dagger}(t')\rangle = (\bar{n}_{\mathrm{th}}^j + 1)\delta(t - t')$, where the mean thermal phonon numbers at temperature T are given by $\bar{n}_{\mathrm{th}}^j = (e^{\hbar\omega_{m_j}/k_BT} - 1)^{-1}$, with k_B the Boltzmann constant.

Now we choose the detunings

$$\Delta_{a_1} = -\Delta_{b_1} = -\omega_{m_1}, \quad \Delta_{a_2} = -\Delta_{b_2} = \omega_{m_2}; \quad (4)$$

i.e., cavity modes a_1 and b_2 are pumped by the blue sidebands of the lasers, while modes a_2 and b_1 are driven by the red sidebands, as illustrated in Fig. 1(b). Therefore, the pump

frequencies ν_{x_j} should satisfy

$$\nu_{a_1} - \nu_{a_2} = (\omega_{m_1} + \omega_{m_2}), \tag{5a}$$

$$\nu_{b_1} - \nu_{b_2} = -(\omega_{m_1} + \omega_{m_2}). \tag{5b}$$

With the above choices of detunings, by performing the transformations $z_j \to z_j e^{-i\Delta_{z_j}t}$, $z_j^{\rm in}(t) \to z_j^{\rm in}(t)e^{-i\Delta_{z_j}t}(z = a,b)$, $c_j \to c_j e^{-i\omega_{m_j}t}$, and $c_j^{\rm in}(t) \to c_j^{\rm in}(t)e^{-i\omega_{m_j}t}$, and neglecting fast oscillating terms proportional to $e^{\pm i(\omega_{m_1}+\omega_{m_2})t}$, the Langevin equations, (2), reduce to

$$\dot{a}_1 = -\kappa_{a_1}a_1 - ig_{a_1}c_1^\dagger + \sqrt{2\kappa_{a_1}}a_1^{\rm in}(t), \tag{6a}$$

$$\dot{b}_1 = -\kappa_{b_1}b_1 - ig_{b_1}c_1 + \sqrt{2\kappa_{b_1}}b_1^{\rm in}(t), \tag{6b}$$

$$\dot{a}_2 = -\kappa_{a_2}a_2 - ig_{a_2}c_2 - 2\sqrt{\eta_a\kappa_{a_1}\kappa_{a_2}}a_1 + \sqrt{2\eta_a\kappa_{a_2}}a_1^{\rm in}(t) + \sqrt{2(1-\eta_a)\kappa_{a_2}}\tilde{a}_2^{\rm in}(t), \tag{6c}$$

$$\dot{b}_2 = -\kappa_{b_2}b_2 - ig_{b_2}c_2^\dagger - 2\sqrt{\eta_b\kappa_{b_1}\kappa_{b_2}}b_1 + \sqrt{2\eta_b\kappa_{b_2}}b_1^{\rm in}(t) + \sqrt{2(1-\eta_b)\kappa_{b_2}}\tilde{b}_2^{\rm in}(t), \tag{6d}$$

$$\dot{c}_1 = -\gamma_{m_1}c_1 - ig_{a_1}a_1^\dagger - ig_{b_1}b_1 + \sqrt{2\gamma_{m_1}}c_1^{\rm in}(t), \tag{6e}$$

$$\dot{c}_2 = -\gamma_{m_2}c_2 - ig_{a_2}a_2 - ig_{b_2}b_2^\dagger + \sqrt{2\gamma_{m_2}}c_2^{\rm in}(t). \tag{6f}$$

It should be noted that for our approximations to be valid, we require our system to be in the resolved sideband regime, $\omega_{m_j} \gg \kappa_{z_j}$, as well as to satisfy $\omega_{m_j} \gg g_{z_j}$. The above equations show that in each cavity, the mechanical mode is coupled to the cavity modes via effective parametric amplification as well as beam-splitter-like mixing. While the former interaction leads to photon-phonon entanglement and optical amplification, the latter is damping the mechanical modes. If the coupling strengths satisfy $g_{b_1} > g_{a_1}$ and $g_{a_2} > g_{b_2}$, the optical damping is dominant over amplification and both mechanical oscillators are cooled.

B. Two-mode mechanical entanglement

We can equivalently re-express Eqs. (6) as $\dot{\chi} = \mathcal{Z}\chi + f^{\rm in}(t)$, with the vector $\chi = (x_{a_1},y_{a_1},x_{b_1},y_{b_1},x_{a_2},y_{a_2},x_{b_2},y_{b_2},x_{c_1},y_{c_1},x_{c_2},y_{c_2})^T$, in terms of the quadrature operators defined as $x = (o + o^\dagger)/\sqrt{2}$ and $y = -i(o - o^\dagger)/\sqrt{2}$, while $f^{\rm in}(t)$ contains the corresponding noise operator contributions. The entanglement between the mechanical systems is contained in the 12×12 correlation matrix $\tilde{\sigma}$ given by $\tilde{\sigma}_{ij} = \langle \chi_i\chi_j + \chi_j\chi_i\rangle/2$. In steady-steady state, it satisfies $\mathcal{Z}\tilde{\sigma}_s + \tilde{\sigma}_s\mathcal{Z}^T = -\mathcal{D}$, where D is the noise matrix $\mathcal{D}_{ij}\delta(t-t') = \langle f_i^{\rm in}(t)f_j^{\rm in}(t') + f_j^{\rm in}(t')f_i^{\rm in}(t)\rangle/2$. Since we are only interested in the entanglement between the two mechanical modes, it is enough to consider the reduced correlation matrix σ_{12} related to the two-mode mechanical states. It has the simple structure $\sigma_{12} = \begin{pmatrix} \sigma_{12}^1 & \sigma_{12}^3 \\ (\sigma_{12}^3)^T & \sigma_{12}^2 \end{pmatrix}$, where σ_{12}^1, σ_{12}^2, and σ_{12}^3 are 2×2 matrices containing the autocorrelations of the two systems and their cross-correlations, respectively. The entanglement between the two mechanical modes can be quantified with the logarithmic negativity E_{12} [39], which is defined as

$$E_{12} = \max[0, -\ln(2\zeta_{12})], \tag{7}$$

where ζ_{12} is given in terms of the reduced correlation matrices

$$\zeta_{12} = 2^{-1/2}\sqrt{\Sigma(\sigma_{12}) - \sqrt{\Sigma(\sigma_{12}) - 4{\rm det}\sigma_{12}}}, \tag{8}$$

with $\Sigma(\sigma_{12}) = {\rm det}\sigma_{12}^1 + {\rm det}\sigma_{12}^2 - 2{\rm det}\sigma_{12}^3$.

Solving Eqs. (6) numerically and using Eq. (7) we can investigate the mechanical entanglement in the system. Let us first, however, turn to a regime where we can obtain analytical results. To this end, we consider the cavity dissipation rates $\kappa_{z_j} = \kappa$, the perfect cavity couplings $\eta_z = 1$, and the effective optomechanical couplings

$$g_{a_1} = g_{b_2} = g_1, \quad g_{a_2} = g_{b_1} = g_2. \tag{9}$$

If the cavity dissipation rate is dominating the dynamics of the system, i.e., $\kappa \gg \{g_j, \gamma_{m_j}\bar{n}_{\rm th}^j\}$, the cavity modes follow changes of the mechanical oscillators adiabatically for times $t > 1/\kappa$. In this case we can eliminate the cavity modes and find the simple equations of motion for the mechanical modes c_j,

$$\dot{c}_1(t) = -(\gamma_{m_1} + \tilde{\gamma}_m)c_1(t) + \sqrt{2\gamma_{m_1}}c_1^{\rm in}(t) + \sqrt{2\tilde{\gamma}_m}\tilde{c}_1^{\rm in}(t), \tag{10a}$$

$$\dot{c}_2(t) = -(\gamma_{m_2} + \tilde{\gamma}_m)c_2(t) + \sqrt{2\gamma_{m_2}}c_2^{\rm in}(t) + \sqrt{2\tilde{\gamma}_m}\tilde{c}_2^{\rm in}(t), \tag{10b}$$

where $\tilde{\gamma}_m = (g_2^2 - g_1^2)/\kappa$ is the net optomechanical damping rate. The noise operators $\tilde{c}_j^{\rm in}(t)$ are given by

$$\tilde{c}_1^{\rm in}(t) = -\frac{ig_1}{\sqrt{\kappa\tilde{\gamma}_m}}a_1^{\rm in\dagger}(t) - \frac{ig_2}{\sqrt{\kappa\tilde{\gamma}_m}}b_1^{\rm in}(t), \tag{11a}$$

$$\tilde{c}_2^{\rm in}(t) = \frac{ig_2}{\sqrt{\kappa\tilde{\gamma}_m}}a_1^{\rm in}(t) + \frac{ig_1}{\sqrt{\kappa\tilde{\gamma}_m}}b_1^{\rm in\dagger}(t) \tag{11b}$$

and have nonvanishing correlations

$$\langle \tilde{c}_j^{\rm in\dagger}(t)\tilde{c}_j^{\rm in}(t')\rangle = N_m\delta(t-t'), \tag{12a}$$

$$\langle \tilde{c}_j^{\rm in}(t)\tilde{c}_j^{\rm in\dagger}(t')\rangle = (N_m+1)\delta(t-t'), \tag{12b}$$

$$\langle \tilde{c}_1^{\rm in}(t)\tilde{c}_2^{\rm in}(t')\rangle = \sqrt{N_m(N_m+1)}\delta(t-t'), \tag{12c}$$

with $N_m = g_1^2/(g_2^2 - g_1^2)$. The above correlations indicate that the two mechanical oscillators are effectively coupled to a broadband quantum reservoir in a two-mode squeezed vacuum state [40]. In the absence of the mechanical damping ($\gamma_{m_j} = 0$), the mechanical oscillators will reduce to the state of the reservoir in the long-time limit, i.e., the two-mode squeezed vacuum

$$|\psi\rangle_{12}^{ss} = \exp(-rc_1^\dagger c_2^\dagger + rc_1c_2)|0_{c_1},0_{c_2}\rangle, \tag{13}$$

with the squeezing parameter $r = \tanh^{-1}(g_1/g_2)$ dependent only on the relative strengths of the two pump lasers. Therefore, the strong mechanical entanglement can be built up, in principle, just by controlling the ratio of the strengths of the pump lasers. It should be pointed that our scheme is quite different from that in Ref. [22], which discussed the establishment of the stationary entanglement between two mechanical oscillators by injecting externally squeezed light into the cavities. Here, instead of creating entanglement in an external source, the entanglement between the mechanical

oscillator and the blue-driven cavity mode is created via the parametric interaction in each cavity, and the photon-phonon entanglement is then transferred to the mechanical oscillators with the help of the beam-splitter interaction.

By taking into account mechanical damping, from Eq. (10) we have the steady-state values $\langle c_j^\dagger c_j\rangle = (\gamma_m \bar{n}_{\rm th} + \tilde{\gamma}_m N_m)/(\gamma_m + \tilde{\gamma}_m)$ and $\langle c_1 c_2\rangle = \tilde{\gamma}_m M_m/(\gamma_m + \tilde{\gamma}_m)$, where we have assumed $\gamma_{m_1} = \gamma_{m_2} \equiv \gamma_m$ and $\bar{n}_{\rm th}^1 = \bar{n}_{\rm th}^2 \equiv \bar{n}_{\rm th}$ for simplicity. It is easy to find the entanglement parameter

$$\zeta_{12} = \frac{1}{2} - \frac{g_1(g_2 - g_1) - \kappa\gamma_m \bar{n}_{\rm th}}{\kappa\gamma_m + g_2^2 - g_1^2}. \tag{14}$$

Clearly, the steady-state mechanical entanglement can be achieved at nonzero temperature, provided that the mean number of thermal phonons satisfies

$$\bar{n}_{\rm th} < \frac{g_1 g_2}{\kappa\gamma_m}\left(1 - \frac{g_1}{g_2}\right). \tag{15}$$

Given that the couplings g_j are tunable through the pump lasers, this condition demonstrates the robustness of steady-state entanglement against thermal noise in the mechanical systems.

We next turn to the numerical results from solving Eqs. (6), which allows us to investigate the entanglement property in the regime where the adiabatical elimination of the cavity modes is invalid. In Fig. 2 the dependence of steady-state mechanical entanglement on the cavity decay rate κ is plotted for different values of g_2/g_1 and the mechanical damping $\gamma_m = 0$. Consistently with our analytic results we observe that, for large cavity decay $\kappa \gg g_j$, the entanglement becomes saturated and independent of κ. The increase in the entanglement with decreasing coupling ratios g_2/g_1 is also evident in this regime. Furthermore, for the opposite situation $\kappa \ll g_j$, we also observe the steady-state entanglement, although to a smaller degree than in the adiabatic regime. The behavior of the steady-state entanglement in the presence of mechanical

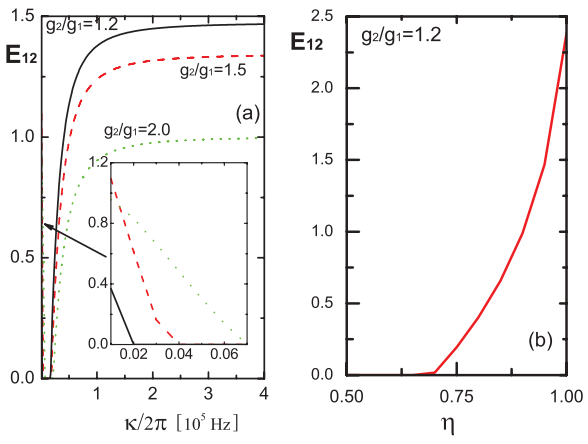

FIG. 2. (Color online) (a) Dependence of the steady-state mechanical entanglement E_{12} on the cavity dissipation rate κ for different coupling ratios g_2/g_1. Other parameters are the mechanical decay rate $\gamma_m = 0$, the coupling strength $g_1/2\pi = 0.1 \times 10^5$ Hz, and the unidirectional intercavity coupling efficiency $\eta = 0.95$. (b) The mechanical entanglement as a function of the coupling efficiency η for the relative strength $g_2/g_1 = 1.2$ and the other parameters are the same as in (a).

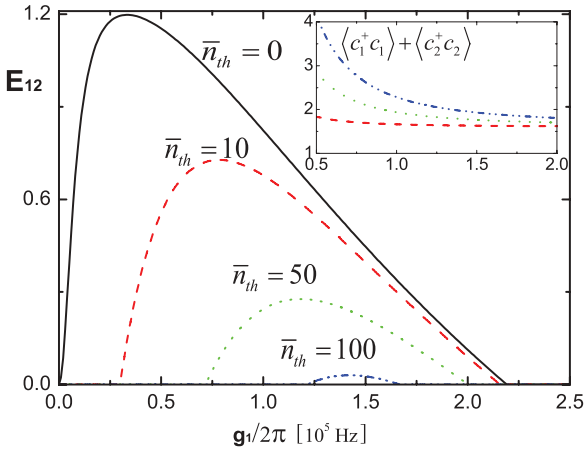

FIG. 3. (Color online) Dependence of the mechanical entanglement on the coupling g_1 for different values of mean thermal phonon number $\bar{n}_{\rm th}$, with the cavity decay rate $\kappa/2\pi = 4 \times 10^5$ Hz, mechanical damping rate $\gamma_m/2\pi = 100$ Hz, coupling $g_2 = 1.5g_1$, and unidirectional coupling efficiency $\eta = 0.95$.

damping is demonstrated in Fig. 3. We see that in this case the optimal entanglement does not occur in the adiabatical regime. With increasing thermal phonon number $\bar{n}_{\rm th}$, stronger coupling strengths g_j are needed to achieve the maximum entanglement. However, the robustness of the generated entanglement is obvious, as it can still be maintained for a relatively high mean thermal phonon number $\bar{n}_{\rm th} = 100$. Reaching the quantum ground state of the vibrational modes is therefore not a prerequisite of the present scheme, which reduces experimental difficulties considerably.

C. Equivalent master equations

It is instructive to discuss the master equation for the systems density operator $\rho(t)$ which corresponds to the Langevin equations, (6), to gain insight into the physical mechanism behind the scheme. It reads

$$\frac{d\rho(t)}{dt} = -i[H_{\rm eff},\rho] + \sum_j \mathcal{L}_\kappa[a_j]\rho + \mathcal{L}_\kappa[b_j]\rho + \mathcal{L}_\gamma[c_j]\rho + \mathcal{L}_c[a_1,a_2]\rho + \mathcal{L}_c[b_1,b_2]\rho, \tag{16}$$

where the effective linearized optomechanical Hamiltonian,

$$H_{\rm eff} = (g_{a_1}a_1 + g_{b_1}b_1^\dagger)c_1 + (g_{a_2}a_2^\dagger + g_{b_2}b_2)c_2 + \text{H.c.}, \tag{17}$$

and the damping terms,

$$\mathcal{L}_\kappa[\mathcal{O}]\rho = \kappa_\mathcal{O}[\mathcal{O},\rho\mathcal{O}^\dagger] + \text{H.c.}, \tag{18a}$$

$$\mathcal{L}_\gamma[c_j]\rho = \gamma_{m_j}(\bar{n}_{\rm th}^j + 1)[c_j,\rho c_j^\dagger] + \gamma_{m_j}\bar{n}_{\rm th}^j[c_j^\dagger,\rho c_j] + \text{H.c.}, \tag{18b}$$

$$\mathcal{L}_c[\mathcal{O}_1,\mathcal{O}_2]\rho = 2\sqrt{\eta_\mathcal{O}\kappa_{\mathcal{O}_1}\kappa_{\mathcal{O}_2}}[\mathcal{O}_1,\rho\mathcal{O}_2^\dagger] + \text{H.c.}, \tag{18c}$$

where $\mathcal{O} \in \{a,b\}$. The dissipative terms $\mathcal{L}_\kappa[\mathcal{O}]\rho$ and $\mathcal{L}_\gamma[c_j]\rho$ describe the damping of the cavity in vacuum and the mechanical modes in thermal environments, while the cross terms $\mathcal{L}_c[\mathcal{O}_1,\mathcal{O}_2]\rho$ account for the unidirectional couplings between the corresponding cavity modes. According to the master equation, (16), the generation of the mechanical entanglement can be understood as follows. Via the parametric amplification

described in Eq. (17), the optomechanical entanglement between the blue-driven cavity modes and the mechanical modes can be built up. By the unidirectional couplings between the cavity modes and the beam-splitter-like interactions involving the red-driven cavity modes and mechanical modes, the optomechanical entanglement is distributed among the two mechanical oscillators and mechanical entanglement is therefore achieved. The two entanglement channels interfere constructively with each other, which leads to stronger mechanical entanglement compared to the single-channel case. In addition, the present two-channel scheme can also avoid the phonon heating from the parametric amplification, through the beam-splitter-like interactions.

Eliminating the cavity modes, as we have done before, leads to the effective master equation for the density matrix ρ_c involving only the mechanical modes c_1 and c_2,

$$\frac{d\rho_c(t)}{dt} = \mathcal{L}[c_1,c_2]\rho_c + \sum_j \mathcal{L}_\gamma[c_j]\rho_c, \tag{19}$$

where the dissipation term

$$\begin{aligned}\mathcal{L}[c_1,c_2]\rho_c = &\sum_j \tilde{\gamma}_m(N_m+1)[c_j,\rho_c c_j^\dagger] + \tilde{\gamma}_m N_m[c_j^\dagger,\rho_c c_j] \\ &+ \tilde{\gamma}_m\sqrt{N_m(N_m+1)}([c_1,\rho_c c_2] + [c_1^\dagger,\rho_c c_2^\dagger]) \\ &+ \text{H.c.}\end{aligned} \tag{20}$$

The above master equation, (19), is equivalent to the Langevin equation, (10), and the dissipative term $\mathcal{L}[c_1,c_2]\rho_c$ characterizes the coupling of the two mechanical modes to a correlated phononic reservoir in a two-mode squeezed vacuum [the correlations are embodied in the second line in Eq. (20)]. This reservoir with nonclassical correlations is achieved by engineering the appropriate interactions between the mechanical modes and the cavity modes with strong dissipation rates. For the engineered dissipative process $\mathcal{L}[c_1,c_2]$, we have

$$\mathcal{L}[c_1,c_2]\left(|\psi\rangle_{12}^{ss}\langle\psi|\right) = 0; \tag{21}$$

i.e., for the negligible mechanical damping ($\gamma_m = 0$) the mechanical modes dissipate toward a pure and stationary two-mode mechanical squeezed vacuum, independent of the effective damping $\tilde{\gamma}_m$.

III. MULTIPARTITE MECHANICAL ENTANGLEMENT

In this section, we generalize the previous two-cavity model to a system of N mechanical oscillators in coupled cavities, as shown in Fig. 4, and proceed to discuss the generation

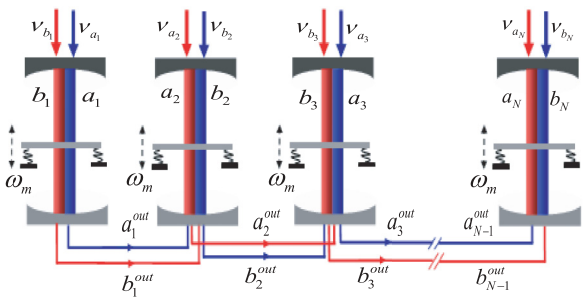

FIG. 4. (Color online) Schematic of N vibrating membranes trapped in cascaded cavities.

of multipartite mechanical entanglement. Consistent with the previous model, we also introduce the convention that the cavity modes a_{2n-1} and b_{2n} are driven by the blue sidebands of the pump lasers, while a_{2n} and b_{2n-1} are driven by the red sidebands, as depicted in Fig. 4. Assuming identical mechanical frequencies (ω_m) for all oscillators and also identical frequencies of cavity modes a_N and b_N, we thus have the effective detuning

$$\Delta_{a_{2n-1}} = -\Delta_{b_{2n-1}} = -\omega_m, \quad \Delta_{a_{2n}} = -\Delta_{b_{2n}} = \omega_m \tag{22}$$

and the driving frequencies

$$\nu_{a_{2n}} - \nu_{a_{2n-1}} = -2\omega_m, \quad \nu_{b_{2n}} - \nu_{b_{2n-1}} = 2\omega_m. \tag{23}$$

With the same procedures and approximations as before, the Langevin equations of motion for cavity modes $z_j (z = a,b)$ and mechanical modes c_j can be obtained and read:

$$\begin{aligned}\dot{z}_j = &-\kappa_z z_j - ig_z c_j^z - 2\kappa_z\sum_{s=1}^{j-1}(\sqrt{\eta_z})^{j-s}z_s \\ &+ \sqrt{2\kappa_z}\sum_{s=2}^{j}\sqrt{\eta_z^{j-s}(1-\eta_z)}\tilde{z}_s^{\text{in}}(t) \\ &+ \sqrt{2\kappa_z}(\sqrt{\eta_z})^{j-1}z_1^{\text{in}}(t),\end{aligned} \tag{24a}$$

$$\dot{c}_j = -\gamma_m c_j - ig_a a_j^x - ig_b b_j^x + \sqrt{2\gamma_m}c_j^{\text{in}}(t), \tag{24b}$$

where the symbols are

$$\left(g_a,g_b,c_j^a,c_j^b,a_j^x,b_j^x\right) = \begin{cases}(g_1,g_2,c_j^\dagger,c_j,a_j^\dagger,b_j) & \text{for} \quad j \text{ odd}, \\ (g_2,g_1,c_j,c_j^\dagger,a_j,b_j^\dagger) & \text{for} \quad j \text{ even},\end{cases}$$

with the optomechanical couplings $g_{a_{2n-1}} = g_{b_{2n}} = g_1$ and $g_{b_{2n-1}} = g_{a_{2n}} = g_2$. The local vacuum noise operators are denoted $\tilde{z}_s(t)$; the optical and mechanical damping rates, κ_z and γ_m, respectively; and the cavity coupling efficiencies, η_z. Before we turn to the numerical solutions, let us first consider the situation that $\kappa_z \gg \{g_j,\gamma_m\bar{n}_{\text{th}}\}$, which allows us to adiabatically eliminate the cavity modes. For the perfect intercavity couplings $\eta_z = 1$ and identical cavity loss rates $\kappa_z = \kappa$, the equations of motion for the odd and even mechanical oscillators are

$$\begin{aligned}\dot{c}_{2n-1}(t) = &-(\gamma_m+\tilde{\gamma}_m)c_{2n-1}(t) - 2\tilde{\gamma}_m\sum_{s=1}^{n-1}c_{2s-1}(t) \\ &+ \sqrt{2\gamma_m}c_{2n-1}^{\text{in}}(t) + \sqrt{2\tilde{\gamma}_m}\tilde{c}_1^{\text{in}}(t),\end{aligned} \tag{25a}$$

$$\begin{aligned}\dot{c}_{2n}(t) = &-(\gamma_m+\tilde{\gamma}_m)c_{2n}(t) - 2\tilde{\gamma}_m\sum_{s=1}^{n-1}c_{2s}(t) \\ &+ \sqrt{2\gamma_m}c_{2n}^{\text{in}}(t) + \sqrt{2\tilde{\gamma}_m}\tilde{c}_2^{\text{in}}(t).\end{aligned} \tag{25b}$$

From the above equations we see that the odd and even mechanical oscillators are coupled to the noise operators $\tilde{c}_1^{\text{in}}(t)$ and $\tilde{c}_2^{\text{in}}(t)$, respectively. Therefore, the entanglement may be established between any odd and even mechanical oscillators, with the nonclassical correlations between the noises $\tilde{c}_1^{\text{in}}(t)$ and $\tilde{c}_2^{\text{in}}(t)$ given in Eq. (12). However, between the oscillators with the same parity, quantum entanglement cannot be established. This is because the source of entanglement in this scheme results from the coupling of the red sideband output to the blue

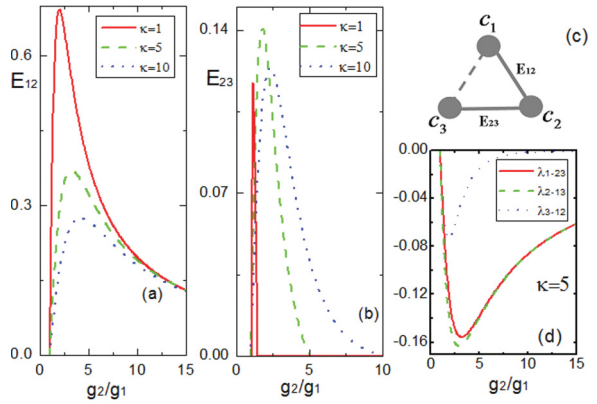

FIG. 5. (Color online) (a) The steady-state reduced bipartite entanglement E_{12} between mechanical modes c_1 and c_2 and (b) the reduced bipartite entanglement E_{23} between modes c_2 and c_3 for a three-mode mechanical system. (c) The tripartite entanglement structure of the mechanical oscillators; solid lines represent reduced bipartite entanglement. (d) Plot depicting the negative eigenvalues of the partially transposed correlation matrix of the three-mode mechanical system with respect to any one mechanical mode, which demonstrates that genuine tripartite mechanical entanglement can be achieved. The unit of κ is 10^5 Hz, the coupling strength $g_1/2\pi = 0.01 \times 10^5$ Hz, the mechanical rate $\gamma_m/2\pi = 10$ Hz, the mean thermal phonon number $\bar{n}_{\rm th} = 0$, and the intercavity coupling efficiency $\eta = 1.0$.

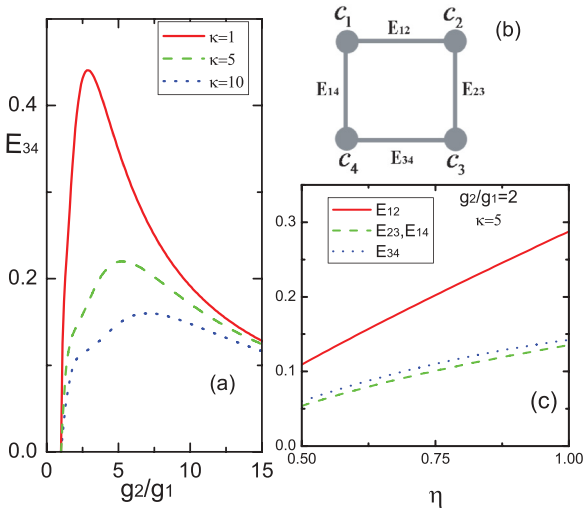

FIG. 6. (Color online) (a) Steady-state bipartite entanglement between mechanical modes c_3 and c_4 for a four-mode mechanical system. (b) Quadripartite square graph-state entanglement among the four remote mechanical oscillators. (c) Dependence of the reduced bipartite entanglement on the intercavity coupling efficiency η. Other parameters used are the same as in Fig. 4.

sideband input, and vice versa. For two even or odd oscillators, the cavity modes coupled to these two oscillators have the same detunings from the pump lasers, which leads them not to entanglement but to mode coupling through an incoherent exchange interaction with rate $-2\tilde{\gamma}_m$. These results are verified in the following via numerical solution of Eqs. (24).

For $N = 3$, we plot in Figs. 5(a) and 5(b) the bipartite entanglement E_{12} between mechanical modes c_1 and c_2 and the bipartite entanglement E_{23} of modes c_2 and c_3, respectively. We see that the entanglement $E_{12} > E_{23}$ for the same parameters. As predicted above, the bipartite entanglement between mechanical modes c_1 and c_3 is absent. Nevertheless, as demonstrated in Fig. 5(d), full inseparable (genuine) tripartite entanglement can be established among the three remote mechanical oscillators. Figure 5(d) depicts the negative eigenvalues λ_{l-mn} of the partially transposed three-mode correlation matrix with respect to the lth mode. The appearance of a negative eigenvalue confirms bipartite entanglement between the transposed mode l and the subsystem of the remaining modes m and n, and fully inseparable (genuine) multipartite entanglement is demonstrated in the regime where the negative eigenvalues simultaneously exist for $l = 1,2,3$ [41]. Also, Fig. 5(d) shows that bipartite entanglement between mode c_2 and the remaining two modes, c_1 and c_3, is largest, since it is the only mode which is simultaneously entangled with the other two subsystems, c_1 and c_3. Finally, the entanglement between mode c_3 and the subsystem including c_1 and c_2 is smallest, since the bipartite entanglement satisfies $E_{23} < E_{12}$ and $E_{13} = 0$. Therefore we see that the negativities will satisfy $\lambda_{3-12} > \lambda_{1-23} > \lambda_{2-13}$.

Extending the above three-mode mechanical system to the four-mode case, i.e., $N = 4$, it is not difficult to see from Eq. (24) that the reduced bipartite entanglements E_{12} and E_{23} are not affected due to the unidirectional cavity coupling. Therefore, the entanglements E_{12} and E_{23} are the the same as in the $N = 3$ case plotted in Fig. 5. Furthermore, it can be inferred from Eq. (25) that the bipartite entanglements will satisfy $E_{14} = E_{23}$ in the bad-cavity limit. In Fig. 6(a), we plot the bipartite entanglement E_{34} between mechanical modes c_3 and c_4, and it is obvious that it exhibits behavior similar to that of entanglement E_{12} between modes c_1 and c_2 (see Fig. 5). We therefore see that quadripartite square graph-state entanglement among four remote mechanical oscillators can be achieved via cascaded cavity couplings. This kind of multipartite entanglement is useful in the field of long-distance quantum communication. The effects of imperfect cavity couplings are illustrated in Fig. 6(c). We see that for a coupling efficiency as low as $\eta = 0.5$, genuine quadripartite entanglement of four distant mechanical oscillators can still be achieved.

IV. CONCLUSION

In conclusion, we propose a scheme to generate steady-state entanglement of remote mechanical oscillators in unidirectionally coupled cavities in a cascaded way. We note here that while the present model assumes the membranes to be mechanical oscillators, the role of mechanical elements can also be played by momentum modes of clouds of ultracold atoms. By choosing the detuning of the pump lasers, in each cavity the mechanical oscillator is coupled to the two cavity modes via parametric and beam-splitter-like interactions. The output quantum fluctuating field of the first cavity subsequently drives the second cavity with reversed detunings. For the case of two mechanical oscillators in cascaded cavities, strong cavity dissipation can pull the two mechanical oscillators into a stationary two-mode squeezed vacuum state for negligible mechanical damping. Two-mode mechanical entanglement

depends on the relative strength of the pump lasers and is robust to thermal fluctuations. For multiple mechanical oscillators in multiple cascaded cavities, it is found that steady-state bipartite entanglement can be established between the odd and the even oscillators, whereas odd and even oscillators do not become entangled. We show that, using this scheme, genuine multipartite entanglement can be achieved among remote mechanical oscillators by cascaded cavity coupling. This kind of remote multipartite macroscopic entanglement is a useful resource in the construction of long-distance quantum communication networks.

ACKNOWLEDGMENTS

B.F.B. and H.S. acknowledge Pierre Meystre for his ongoing support. This work is supported by the National Natural Science Foundation of China (Grants No. 11274134, No. 11074087, and No. 61275123), the National Basic Research Program of China (Grant No. 2012CB921602), the Natural Science Foundation of Hubei Province (Grant No. 2010CDA075), and the Natural Science Foundation of Wuhan City (Grant No. 201150530149). T.H.T. acknowledges the support from the CSC.

[1] W. H. Zurek, Phys. Today **44**, 36 (1991).
[2] M. Poot and H. S. J. van der Zant, Phys. Rep. **511**, 273 (2012).
[3] F. Marquardt and S. M. Girvin, Physics **2**, 40 (2009).
[4] M. Aspelmeyer, S. Groeblacher, K. Hammerer, and N. Kiesel, J. Opt. Soc. Am. B **27**, 189 (2010).
[5] S. Gigan *et al*., Nature **444**, 67 (2006).
[6] T. Corbitt, Y. Chen, E. Innerhofer, H. Muller-Ebhardt, D. Ottaway, H. Rehbein, D. Sigg, S. Whitcomb, C. Wipf, and N. Mavalvala, Phys. Rev. Lett. **98**, 150802 (2007).
[7] J. D. Teufel *et al*., Nature **475**, 359 (2011).
[8] J. Chan *et al*., Nature **478**, 89 (2011).
[9] K. Stannigel, P. Komar, S. J. M. Habraken, S. D. Bennett, M. D. Lukin, P. Zoller, and P. Rabl, Phys. Rev. Lett. **109**, 013603 (2012).
[10] K. Zhang, P. Meystre, and W. P. Zhang, Phys. Rev. Lett. **108**, 240405 (2012).
[11] L. Tian, Phys. Rev. Lett. **108**, 153604 (2012); Y. D. Wang and A. A. Clerk, *ibid*. **108**, 153603 (2012).
[12] L. F. Buchmann, L. Zhang, A. Chiruvelli, and P. Meystre, Phys. Rev. Lett. **108**, 210403 (2012).
[13] P. Rabl, Phys. Rev. Lett. **107**, 063601 (2011); A. Nunnenkamp, K. Børkje, and S. M. Girvin, *ibid*. **107**, 063602 (2011).
[14] M. Ludwig, A. H. Safavi-Naeini, O. Painter, and F. Marquardt, Phys. Rev. Lett. **109**, 063601 (2012).
[15] M. Paternostro, Phys. Rev. Lett. **106**, 183601 (2011).
[16] C. Genes, H. Ritsch, M. Drewsen, and A. Dantan, Phys. Rev. A **84**, 051801(R) (2011).
[17] D. Vitali, S. Gigan, A. Ferreira, H. R. Bohm, P. Tombesi, A. Guerreiro, V. Vedral, A. Zeilinger, and M. Aspelmeyer, Phys. Rev. Lett. **98**, 030405 (2007).
[18] S. Mancini, V. Giovannetti, D. Vitali, and P. Tombesi, Phys. Rev. Lett. **88**, 120401 (2002).
[19] M. Pinard, A. Dantan, D. Vitali, O. Arcizet, T. Briant, and A. Heidmann, Europhys. Lett. **72**, 747 (2005).
[20] M. J. Hartmann and M. B. Plenio, Phys. Rev. Lett. **101**, 200503 (2008).
[21] L. Zhou, Y. Han, J. Jing, and W. P. Zhang, Phys. Rev. A **83**, 052117 (2011).
[22] J. Zhang, K. Peng, and S. L. Braunstein, Phys. Rev. A **68**, 013808 (2003).
[23] S. Pirandola, D. Vitali, P. Tombesi, and S. Lloyd, Phys. Rev. Lett. **97**, 150403 (2006).
[24] K. Børkje, A. Nunnenkamp, and S. M. Girvin, Phys. Rev. Lett. **107**, 123601 (2011).
[25] C. Joshi, J. Larson, M. Jonson, E. Andersson, and P. Öhberg, Phys. Rev. A **85**, 033805 (2012).
[26] H. J. Kimble, Nature **453**, 1023 (2008).
[27] C. A. Muschik, H. Krauter, K. Jensen, J. M. Petersen, J. I. Cirac, and E. S. Polzik, J. Phys. B **45**, 124021 (2012).
[28] S. Clark, A. Peng, M. Gu, and S. Parkins, Phys. Rev. Lett. **91**, 177901 (2003).
[29] A. S. Parkins, E. Solano, and J. I. Cirac, Phys. Rev. Lett. **96**, 053602 (2006).
[30] S. B. Zheng, Z. B. Yang, and Y. Xia, Phys. Rev. A **81**, 015804 (2010).
[31] C. A. Muschik, E. S. Polzik, and J. I. Cirac, Phys. Rev. A **83**, 052312 (2011).
[32] W. L. Yang, Z. Q. Yin, Q. Chen, C. Y. Chen, and M. Feng, Phys. Rev. A **85**, 022324 (2012).
[33] G. X. Li, S. S. Ke, and Z. Ficek, Phys. Rev. A **79**, 033827 (2009); L. H. Sun, Y. Q. Chen, and G. X. Li, Opt. Express **20**, 3176 (2012).
[34] H. Krauter, C. A. Muschik, K. Jensen, W. Wasilewski, J. M. Petersen, J. I. Cirac, and E. S. Polzik, Phys. Rev. Lett. **107**, 080503 (2011).
[35] C. W. Gardiner and P. Zoller, in *Quantum Noise* (Springer, Berlin, 2004).
[36] J. D. Thompson *et al*., Nature **452**, 72 (2008).
[37] M. Bhattacharya and P. Meystre, Phys. Rev. A **78**, 041801(R) (2008).
[38] F. Brennecke, S. Ritter, T. Donner, and T. Esslinger, Science **322**, 235 (2008); H. Jing, D. S. Goldbaum, L. Buchmann, and P. Meystre, Phys. Rev. Lett. **106**, 223601 (2011).
[39] G. Vidal and R. F. Werner, Phys. Rev. A **65**, 032314 (2002).
[40] P. Meystre and M. Sargent III, in *Elements of Quantum Optics*, 4th ed. (Springer, Berlin, 2007).
[41] G. Giedke, B. Kraus, M. Lewenstein, and J. I. Cirac, Phys. Rev. A **64**, 052303 (2001).